Bilateral Comparison of 10 V Standards between the NSAI - NML (Ireland) and the BIPM,

December 2020

(part of the ongoing BIPM key comparison BIPM.EM-K11.a and b)

by S. Solve[+], R. Chayramy[+], O. Power* and M. Stock[+]

[+] Bureau International des Poids et Mesures, BIPM, Sèvres, France

* National Standards Authority of Ireland - National Metrology Laboratory

(NSAI - NML), Dublin, Ireland

Introduction

As part of the ongoing BIPM key comparison BIPM.EM-K11, a comparison of the 10 V voltage reference standards of the BIPM and the National Standards Authority of Ireland – National Metrology Laboratory (NSAI - NML)**,** Dublin, Ireland, was carried out in November and December 2020. The objective for NSAI-NML in participating in this comparison was to demonstrate the international equivalence of its DC voltage measurement results and to support their calibration and measurement capabilities (CMCs) published in the Key Comparison Database of the BIPM (KCDB).

Two BIPM Zener diode-based travelling standards (Fluke 732B), BIPM_8 (Z8) and BIPM_9 (Z9), were transported by freight to NSAI-NML. At NSAI-NML, the reference standard for DC voltage at the 10 V level consists of a group of characterized Zener diode-based electronic voltage standards. The output EMF (Electromotive Force) of each travelling standard was measured by direct comparison with the group standard.

At the BIPM the travelling standards were calibrated, before and after the measurements at NSAI-NML, with the Josephson Voltage Standard, developed at the BIPM. The output EMF of each travelling standard was measured against the Josephson Voltage Standard (JVS). Results of all measurements were corrected for the dependence of the output voltages of the Zener standards on internal temperature and ambient atmospheric pressure.

This report presents the results of the comparison of the calibrations of the two travelling Zener standards at 10 V.

Outline of the measuring method

NSAI-NML 10 V measurements

The EMF at the 10 V output terminals of the travelling standard is connected in series opposition to each individual member of the NSAI-NML group standard in turn, using a low thermal EMF scanner. The EMF differences are measured using a digital nanovoltmeter. The measured voltage differences, together with the predicted values of the NSAI-NML standards are subjected to a weighted least squares adjustment procedure in order to arrive at a best estimate of the unknown EMF.

BIPM 10 V measurements

The output voltage of the Zener standard to be measured is connected in series opposition to the BIPM Josephson Voltage Standard - *Hypres* 10 V SIS array (S/N: 2538F-3), through a low thermal EMF switch. The binding post terminals “GUARD” and “CHASSIS” of the Zener standard are connected together to a single point which is the grounding reference point of the measurement setup and which is a dedicated instrument earth potential.

The measurements start at least two hours after the mains power plug at the rear of the Zeners has been disconnected in order for the Zener internal temperature to stabilize.

The BIPM detector consists of an EM model N1a analog nanovoltmeter whose output is connected, via an optically-coupled isolation amplifier, to a digital voltmeter (DVM) which is connected to a computer.

This computer is used to monitor measurements, acquires data and calculates results. Low thermal EMF switches are used for critical switching, such as polarity reversal of the detector input.

The BIPM array biasing frequency has been adjusted to a value where the voltage difference between the primary and the secondary voltage standards is below 1 µV for both nominal voltages. The nanovoltmeter is set to its 10 µV range for the measurements performed at the level of 10 V.

One individual measurement point is acquired according to the following procedure:

1- Positive array polarity and positive polarity of the Zener standard. Data acquisition with the + of the detector on the Zener negative polarity side;

2- Data acquisition with the detector reversed (+ of the detector on the array negative polarity side);
3- Negative array polarity and negative polarity of the Zener standard. Data acquisition with the + of the detector on the Zener positive polarity side;
4- Data acquisition with the detector reversed (+ of the detector on the array positive polarity side);
5- Data acquisition with the + of the detector on the Zener positive polarity side;
6- Data acquisition with the detector reversed (+ of the detector on the array positive polarity side);
7- Positive array polarity and positive polarity of the Zener standard. Data acquisition with the + of the detector on the Zener negative polarity side;
8- Data acquisition with the detector reversed (+ of the detector on the array negative polarity side).

The reversal of the array polarity (by reversing the bias current) is always accompanied by a reversal of the Zener voltage standard using a switch. The reversal of the detector polarity is done to cancel out any detector internal thermal EMF with linear time-dependence and to check that there is no AC voltage noise rectified at the input of the detector (this is the case if the reading is different in the positive and negative polarity of the analog detector by up to a few hundred microvolts).

Each data acquisition step consists of 30 preliminary points followed by 500 measurement points. Each of these should not differ from the mean of the preliminary points by more than twice their standard deviation, if so, the software warns the operator with a beep. If too many beeps occur (typically 10), the operator can reject the data acquisition sequence and start it again. Each data acquisition sequence lasts 25 s and the array must remain on its quantum voltage step during this period of time. The total measurement time (including polarity reversals and data acquisition) is approximately 5 minutes.

This procedure is repeated three times and the mean value corresponds to one result on the graph (cf. Figs. 1 and 2).

Results at 10 V

Figure 1 shows the measured values obtained for the two standards by the two laboratories at 10 V. Figure 2 presents the voltage evolution of the arithmetic mean of the two standards which is used to compute the final result at 10 V.

A linear least-squares fit is applied to the results of the BIPM, before and after the measurements at the NSAI-NML, to obtain the results for both standards and their uncertainties at the mean date of the NSAI-NML measurements (14/11/2020).

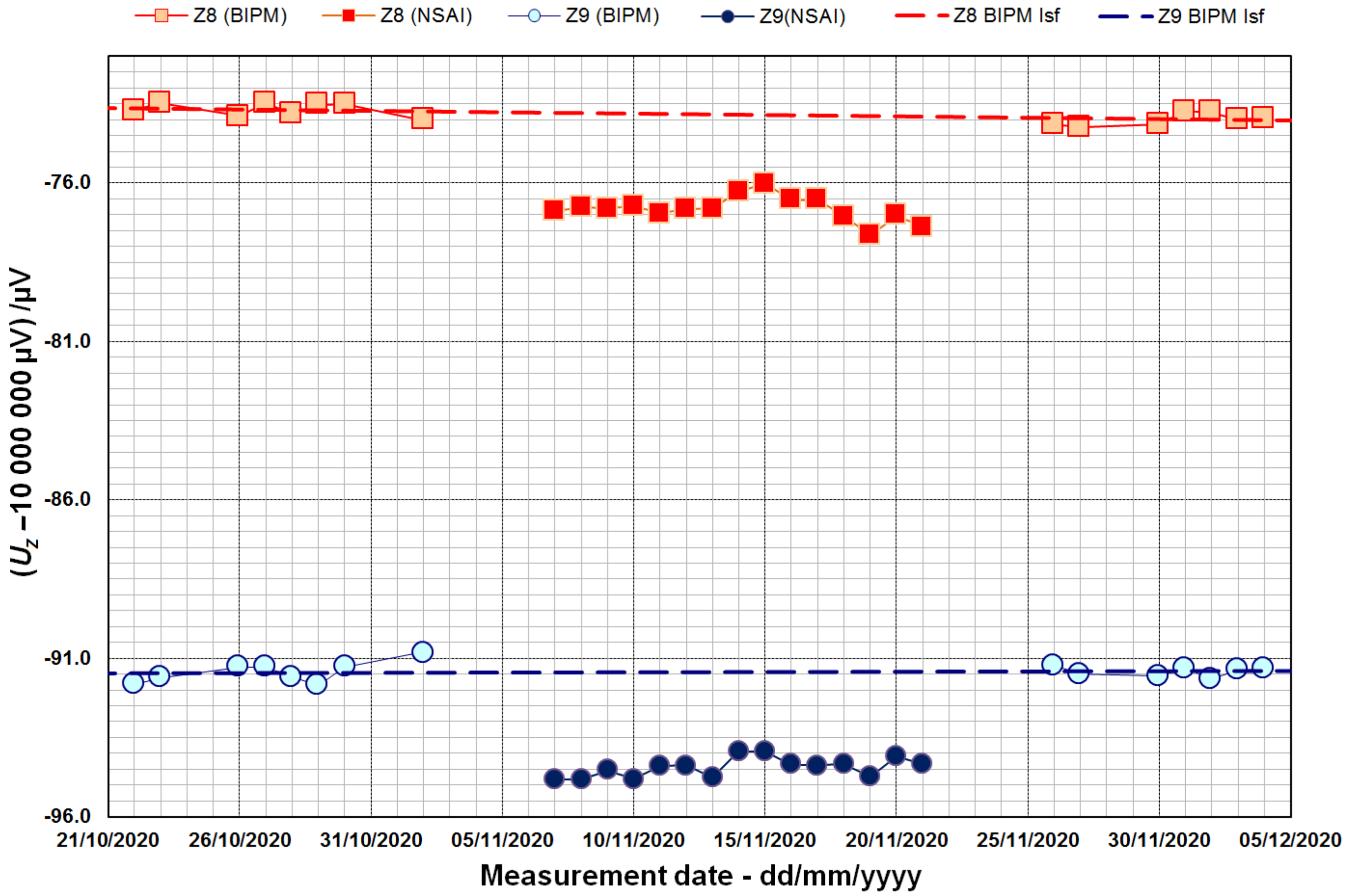

Figure 1: Voltage of Z8 (squares) and Z9 (disks) at 10 V measured at both institutes (light markers for BIPM and dark markers for NSAI-NML), referred to 10 V, as a function of the measurement date with a linear least-squares fit (lsf) to the BIPM measurements**.**

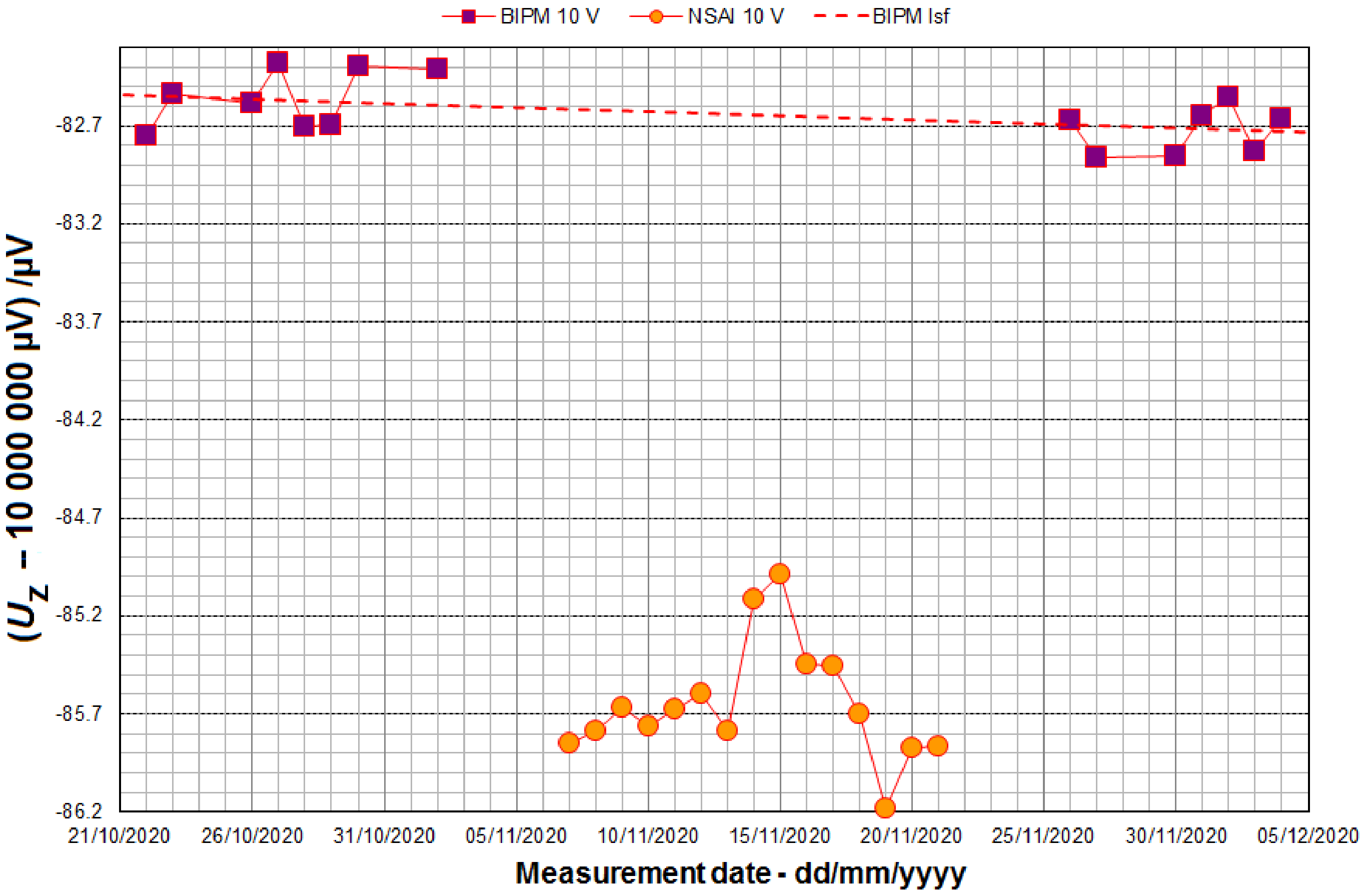

Figure 2: Voltage evolution of the arithmetic mean of the two standards at 10 V. NSAI-NML measurements are represented by disks and BIPM measurements by squares. A least-squares fit is applied to the BIPM measurements.

Uncertainty Budgets at 10 V

BIPM uncertainty budget at 10 V

Table 1 summarizes the uncertainties related to the calibration of a Zener diode against the Josephson array voltage standard at the BIPM at the level of 10 V.

Experience has shown that flicker or 1/*f* noise ultimately limits the stability characteristics of Zener diode standards and it is not appropriate to use the standard deviation divided by the square root of the number of observations to characterize the dispersion of measured values. For the present standards, the relative value of the voltage noise floor due to flicker noise is about 1.5 part in 10^8 [1]. The Type A standard uncertainty in the Table 1 therefore has a lower limit of 150 nV. However, if the standard deviation of the measurements at the mean date of the participant is larger than the flicker noise floor, it is this standard deviation which is considered to be the Type A standard uncertainty.

JVS & detector uncertainty components	**Uncertainty/nV**
Noise of the measurement loop that includes the residual thermal EMF including the residual EMF of the reversing switch	0.86
Detector gain (Type B)	0.11
Leakage resistance (Type B)	0.03
Frequency (Type B)	0.03
Zener noise (Type A)	Not lower than the 1/*f* noise estimated as 150 nV, included in the comparison uncertainty budget (Table 3)
Zener pressure and temperature correction	Included in the comparison uncertainty budget (Table 3)

Table 1: Estimated standard uncertainties arising from the JVS and the measurement setup for Zener calibrations with the BIPM equipment at the level of 10 V.

NSAI-NML uncertainty budget at 10 V

Table 2 lists the uncertainties related to the calibration of the Zeners at the NSAI-NML. Note that the uncertainty of the temperature and pressure corrections (in italic) are given as an indication only and do not contribute to the final uncertainty budget used for this comparison as they are applied by the BIPM and included in the comparison uncertainty budget (Table 3).

The measurement model is: $U_X = U_{REF} \cdot + f(\delta U_i) + \delta\rho + \delta T$

Input Quantity	Symbol	Standard Uncertainty	Sensitivity Coefficient	Uncertainty Contribution	Note
		(µV)		(µV)	
NSAI-NML Reference	U_{REF}	1.6	1	1.6	(1)
Voltage difference	$f(\delta U_i)$	0.5	1	0.5	(2)
Temperature correction	δ_T	*0.01*	*1*	*0.01*	*(3)*
Pressure Correction	δ_P	*0.03*	*1*	*0.03*	*(4)*
Non-repeatability		0.5	1	0.5	(5)
		Combined Standard Uncertainty		1.75	
		Expanded Uncertainty (*k*=2)		3.5	

Table 2: Estimated standard uncertainties arising from NSAI-NML reference standards and the measurement setup for Zener calibrations with the NSAI-NML equipment at the level of 10 V.

Notes:

(1) The uncertainty component includes the effects of drift, noise, and environmental influences on the ensemble reference standard.
(2) The uncertainty component includes the effects of uncompensated thermal voltage offsets, uncorrected errors in the detector reading, leakage effects, and common mode effects.
(3) A temperature (thermistor resistance) coefficient of 3.5×10^{-7} $k\Omega^{-1}$ is used.
(4) A pressure coefficient of 2×10^{-8} kPa^{-1} is used.
(5) An estimate of the 1/f noise floor level is used as it is greater than the standard deviation of the mean.

Uncertainty contributions for the comparison NSAI-NML/BIPM at 10 V

Table 3 lists the results and the uncertainty contributions for the comparison NSAI-NML/BIPM at 10 V.

The Type A standard uncertainty of the comparison is the quadratic combination of the participants Type A standard uncertainty components. It is included together with the uncertainty on the pressure and temperature corrections in the “uncorrelated uncertainty” component of the Table 3.

		results/µV		**uncertainty/µV**	
		Z8	**Z9**	**Z8**	**Z9**
1	NSAI-NML ($U_{\text{NSAI-NML}}$ – 10 V)	-76.81	-94.44		
2	Type A uncertainty			0.83	0.84
3	correlated (Type B) unc.			1.60	
4	BIPM (U_{BIPM} – 10 V)	-73.84	-91.43		
5	Type A uncertainty			0.15	0.15
6	correlated (Type B) unc.			<0.001	
7	pressure and temperature correction uncertainty			0.00	0.01
8	($U_{\text{NSAI-NML}} – U_{\text{BIPM}}$)	-2.97	-3.01		
9	Total uncorrelated uncertainty			0.84	0.85
10	Total correlated uncertainty			1.60	
11	< $U_{\text{NSAI-NML}} – U_{\text{BIPM}}$ >	**-2.99**			
12	*a priori* uncertainty			0.595	
13	*a posteriori* uncertainty			0.02	
14	**comparison total standard uncertainty/µV**			**1.71**	

Table 3: Results and uncertainties of the NSAI-NML (Ireland)/BIPM bilateral comparison of 10 V standards using two Zener travelling standards: reference date 14 November 2020. Standard uncertainties are used throughout.

In Table 3, the following elements are listed:

(1) the value attributed by NSAI-NML to each Zener $U_{\text{NSAI-NML}}$, computed as the simple mean of all data from NSAI-NML and corrected for temperature and pressure differences between both laboratories by the BIPM.

(2) the NSAI-NML Type A uncertainty (cf. Table 2). This component is calculated as the standard deviation of the mean of the participant measurements once the BIPM has applied the pressure and temperature corrections. As a consequence the Type A uncertainty is different from the one evaluated by the participant.

(3) the uncertainty component arising from the realization and maintenance of the volt at NSAI-NML: it is the quadratic combination of the Type B components of the participant uncertainty budget. This uncertainty is completely correlated between the different Zeners used for the comparison.

(4-6) the corresponding quantities for the BIPM referenced to the mean date of NSAI-NML measurements. In this case, the Type A uncertainty is limited by the flicker noise level of 150 nV.

(7) the comparison uncertainty due to the combined effects of the pressure and temperature coefficients [2-3] and of the differences of the mean pressures and temperatures in the participating laboratories is calculated as follows:

The uncertainty of the temperature correction $u_{T,i}$ of Zener *i* is determined for the difference ΔR_i between the mean values of the thermistor resistances measured at both institutes which is then multiplied by the uncertainties $u(c_{T,i})$ of the relative temperature (thermistor resistance) coefficients of each Zener standard:

$$u_{T,i} = U \times u(c_{T,i}) \times \Delta R_i$$

where U = 10 V, $u(c_{T,Z8})$ = 0.294 × 10^{-7} / kΩ, $u(c_{T,Z9})$ = 0. 231 × 10^{-7} / kΩ and ΔR_{Z8}= 0.006 kΩ and ΔR_{Z9}= 0.049 kΩ. ΔR_{Z8} and ΔR_{Z9} are the difference of the mean values of the thermistor resistance readings at the NSAI-NML and the BIPM.

The same procedure is applied for the uncertainty $u_{P,i}$ on the pressure correction for the difference ΔP_i between the mean values of the pressure measured at both institutes:

$$u_{P,i} = U \times u(c_{P,i}) \times \Delta P_i$$

where U = 10 V, $u(c_{P,Z8})$ = 0.050 × 10^{-9} / hPa, $u(c_{P,Z9})$ = 0.052 × 10^{-9} / hPa, ΔP_{Z8}= 0.4 hPa and ΔP_{Z9}= 0.5 hPa. ΔP_{Z8} and ΔP_{Z9} are the difference of the mean values of the pressures at the NSAI-NML and the BIPM.

The uncertainty on the measurement of the temperature and the pressure are negligible.

(8) the difference ($U_{\text{NSAi-NML}}$ – U_{BIPM}) for each Zener, and (9) the uncorrelated part of the uncertainty, calculated as the quadratic sum of lines 2, 5 and 7.

(10) the correlated part of the uncertainty, calculated as the quadratic sum of lines 3 and 6, for each traveling standard.

(11) the result of the comparison is the simple mean of the differences of the calibration results for the different standards.

(12 and 13) the uncertainty related to the transfer, estimated by comparing the following uncertainties:

(12) the *a priori* uncertainty, determined as the standard uncertainty of the mean, obtained by propagating the uncorrelated uncertainties for both Zeners;
(13) the *a posteriori* uncertainty, which is the standard deviation of the mean of the two results.

(14) the total uncertainty of the comparison, which is the root sum square of the correlated part of the uncertainty (10) and of the larger of (12) and (13).

To estimate the uncertainty related to the stability of the standards during transportation, we have calculated the "*a priori*" uncertainty of the mean of the results obtained for the two standards (also called statistical internal consistency [4]). It consists of the quadratic combination of the uncorrelated uncertainties of each result and is equivalent of the propagation of the uncertainty of each standard. We compared this component to the "*a posteriori*" uncertainty which consists of the experimental standard deviation of the mean of the results from the two travelling standards[1].

If the "*a posteriori*" uncertainty (0.02 µV) would be significantly larger than the "*a priori*" (0.6X µV) uncertainty, we would assume that a standard has changed in an unusual way, probably during its transportation. This is not the case as the BIPM measurements

---

[1] With only two travelling standards, the uncertainty of the standard deviation of the mean is comparable to the value of the standard deviation of the mean itself.

performed before and after the shipment have confirmed. We use the larger of these two estimates in calculating the final uncertainty.

The comparison result is presented as the difference between the value assigned to a 10 V standard by NSAI-NML, at NSAI-NML, $U_{\text{NSAI-NML}}$, and that assigned by the BIPM, at the BIPM, U_{BIPM}, on the reference date of 2020/11/14, as

$$\boldsymbol{U_{\text{NSAI-NML}} - U_{\text{BIPM}} = -2.99\ \mu\text{V};\ \ u_{\text{c}} = 1.71\ \mu\text{V}}$$

where u_{c} is the combined standard uncertainty associated with the measured difference, including the uncertainty of the realization of the volt at NSAI-NML, and the uncertainty related to the comparison.

Conclusion

The final result of the comparison is presented as the difference between the values assigned to DC voltage standards by NSAI-NML, at the level of 10 V, at NSAI-NML, $U_{\text{NSAI-NML}}$, and those assigned by the BIPM, at the BIPM, U_{BIPM}, at the reference dates of the 14th of November 2020.

$$\boldsymbol{U_{\text{NSAI-NML}} - U_{\text{BIPM}} = -2.99\ \mu\text{V};\ u_{\text{c}} = 1.71\ \mu\text{V},\ \text{at}\ 10\ \text{V}}$$

where u_{c} is the combined standard uncertainty associated with the measured difference. This difference appears to be significantly larger than the previous one (-1.21 µV) obtained in 2018. It is more likely that the batch of Zener standards which constitutes the National voltage reference of Ireland has changed an unusual way. It is recommended to calibrate at least one of these standards (preferably all of them) against a primary voltage standard to reestablish the traceability.

References

[1] **Witt T. J.**, Maintenance and dissemination of voltage standards by Zener-diode-based instruments, IEE Proc.-Sci. Meas. Technol., vol. 149, pp. 305-312, 2002.

[2] **Solve S., Chayramy R. and Power O.**, Temperature sensitivity coefficients of the BIPM secondary voltage standards, *CPEM 2016 Digest, Ottawa*,
DOI: 10.1109/CPEM.2016.7540702.

[3] **Solve S., Chayramy R. and Yang S.**, Pressure Sensitivity Coefficients of the BIPM secondary voltage standards, *CPEM 2018 Digest, Paris*:
DOI: 10.1109/CPEM.2018.8501074

[4] **Hoel P. G.**, Introduction to Mathematical Statistics *4th edn*, 1971, New York: Wiley.

ANNEX 1

The BIPM is currently proceeding with the validation process of its automated measurement setup, based on a programmable Josephson Voltage Standard, that will be dedicated to the calibration of the Zener-based voltage standards. The validity process consists of ensuring that the measurements performed with the new system are comparable to the ones performed by the older one within the uncertainties. Therefore, for each standard, we have two measurements on each day in such a way we'd be able to derive two linear fits to the data: the first one with the results of the traditional measurement setup based on the hysteretic array (*Hypres-2538F3*) and the second one with the results of the automated measurement setup based on the PTB programmable array (*SNS-PTB 2013-02/4a*) as shown on Fig. A1.

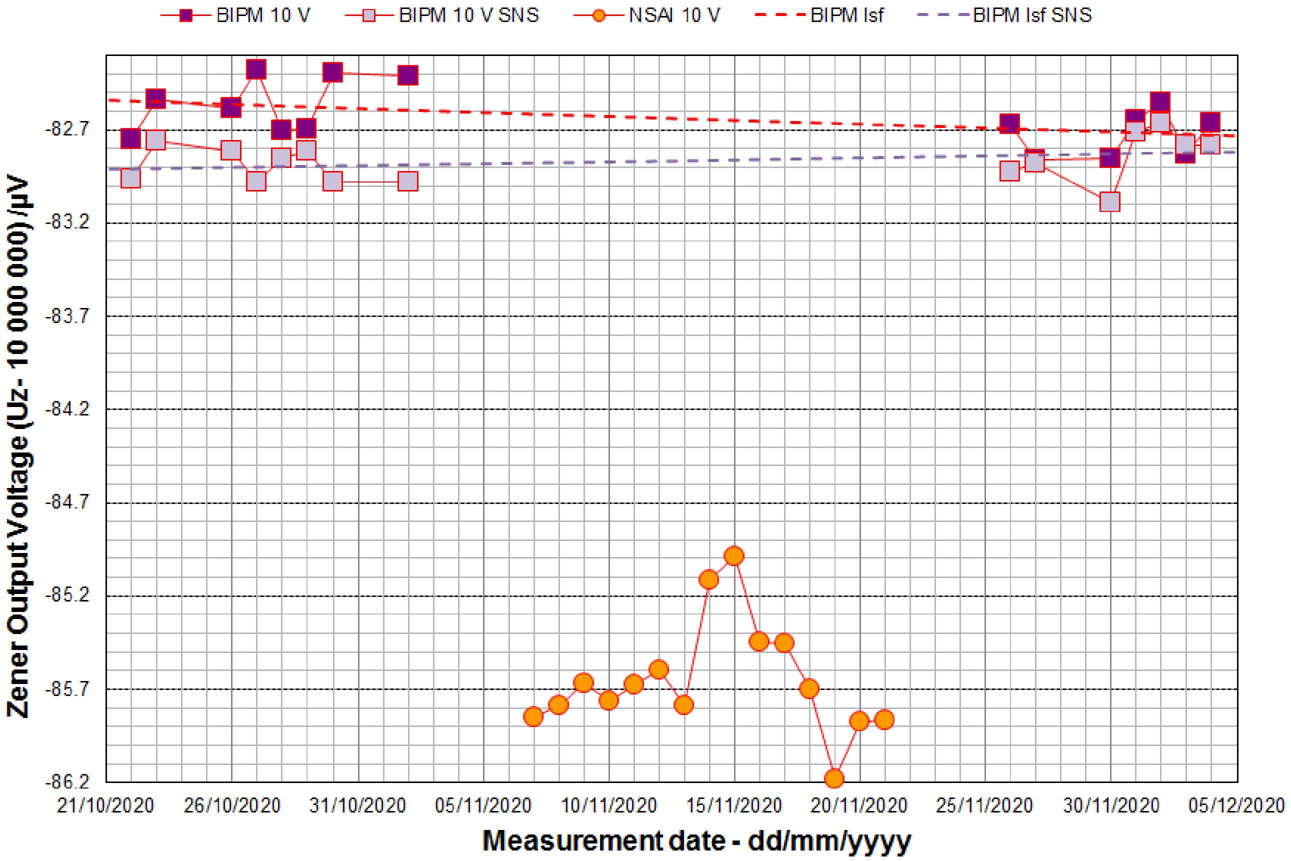

Figure A1. Voltage evolution of the simple mean of the two standards at 10 V.

Figure A1 is a copy of Figure 2 completed by the measurements carried out with the automated measurement setup which are represented by light purple squares.

At the mean time of the NSAI measurements, the comparison result is calculated as the voltage difference between the mean of the NSAI measurements and the result of the fit of the BIPM measurements and is equal to:

$U_{\mathrm{NML}} - U_{\mathrm{BIPM}} = -\,2.99\ \mu\mathrm{V}$, $u_{\mathrm{c}} = 1.71\ \mu\mathrm{V}$, for the official comparison result and

$U_{\mathrm{NML}} - U_{\mathrm{BIPM}} = -\,2.76\ \mu\mathrm{V}$, $u_{\mathrm{c}} = 1.71\ \mu\mathrm{V}$, for the comparison result obtained with the automated measurement setup.

The two results are different by 230 nV and would agree with the BIPM stated uncertainties (for an expansion factor of 2) which are ultimately limited to the 1/*f* noise of 150 nV.

However, if the results are equivalent within the stated comparison uncertainties, Figure A1 shows that the results obtained with the automated setup are always lower than the ones obtained with the traditional setup. From our investigations, the intrinsic physical properties of these particular standards are responsible for this effect. We assume that the difference in the input resistor of the two standards might play a role in the amplitude of the current flowing through in the measurement setup and thus introduce small voltage offsets. We believe that two other devices would have produced a different behaviour but this is to be experimentaly confirmed in a future similar exercise.